Colloid and Polymer Science (2020) 298:1423–1432
https://doi.org/10.1007/s00396-020-04730-4

ORIGINAL CONTRIBUTION

# Synthesis of polyHIPEs through high internal phase emulsions of β-myrcene

E. Hilal Mert[1] · Burcu Kekevi[2]

Received: 16 April 2020 / Revised: 29 July 2020 / Accepted: 12 August 2020 / Published online: 17 August 2020


## Abstract

PolyHIPEs are an important class of porous polymers with well-defined hierarchical porosity and tunable morphology. However, the insufficient mechanical properties arise due to high volume of voids bringing difficulties in applications. In this study, polyHIPEs with tailored morphological and mechanical properties were prepared by using a monoterpene for the first time. In this respect, copolymerization of β-myrcene with several comonomers within water-in-oil (w/o) high internal phase emulsions (HIPEs) has been extensively investigated. Accordingly, combining β-myrcene and ethylene glycol dimethacrylate (EGDMA) in polyHIPE structure was demonstrated as a successful approach for tailoring the morphology, as well as the mechanical strength. PolyHIPEs with cavities between 1.09 and 3.55 μm were obtained by changing the ratio of β-myrcene in the continuous phase of HIPEs. Moreover, resulting polyHIPEs have found to have improved mechanical strength. The highest compressive modulus achieved for the obtained monoliths was determined to be 38.8 MPa.

**Keywords** PolyHIPE · High internal phase emulsion · β-Myrcene · Morphology · Mechanical properties

## Introduction

Poly(high internal phase emulsion)s (polyHIPEs) are an important subclass of porous materials offering many advantages in various fields depending on their hierarchically ordered pore structure [1, 2]. They are generally obtained by polymerization of the continuous phase of water-in-oil (w/o) type high internal phase emulsions (HIPEs) which are containing monomeric species.

HIPEs are concentrated emulsions consisting at least 74 vol% of internal (dispersed) phase. This specified volume ratio is not a random figure. However, it is corresponding to the maximum packing fraction of monodisperse and undeformable spheres [2]. In general, polymerization of a HIPE template is proceeded by free radical polymerization. However, depending on the choice of monomers, different polymerization methods including step growth polymerization [3–5], atom radical transfer polymerization (ATRP) [6], reversible addition-fragmentation chain transfer polymerization (RAFT) [7], and ring opening metathesis polymerization (ROMP) [8, 9] were also adapted to emulsion templating polymerization approach.

Polymerization of the external monomer phase was followed by removal of the internal phase, and the drying steps allow the formation of highly cross-linked, open porous, and low-density monoliths [10, 11]. In general, obtained monoliths have two levels of distinctive topology. In this topology, while the primary macropores are usually termed as cavities or voids, the secondary pores are termed as interconnecting pores, pore throats, or windows [12]. The average size of macropores, which reflects the HIPE droplet size, is determined by the combination of experimental parameters [13] and typically changed between 500 nm and 100 μm. Because of macropore predominance in topology, specific surface area of polyHIPEs is usually lower than 50 $m^2/g$, while their densities are at around of 0.1 $g/cm^3$.

So far, styrene, which has a hydrophobic structure, is the most used monomer for the preparation of polyHIPEs. In most of the studies, divinylbenzene (DVB), another hydrophobic bifunctional monomer, was used as a cross-linker [12, 13]. However, combination of the polymer chains composed of

✉ E. Hilal Mert
hmert@yalova.edu.tr

✉ Burcu Kekevi
bkekevi@yalova.edu.tr

[1] Faculty of Engineering, Department of Polymer Materials Engineering, Yalova University, 77200 Yalova, Turkey

[2] Yalova Community College, Material and Material Processing Department, Yalova University, 77100 Yalova, Turkey

styrene and DVB units, with highly porous structure, usually gives monoliths suffering from brittleness and chalkiness [13–16]. In this respect, several approaches have been developed by researchers to overcome the drawback arisen from low mechanical strength including *(i)* preparation of polyHIPE composites/nanocomposites by incorporating nanoparticles [14, 16–18], *(ii)* increasing monolith density by using lower internal phase emulsions [18, 19], *(iii)* increasing the chain flexibility by incorporating monomers having spacer groups and higher free volume into HIPE templates [15, 19–22], and *(iv)* using monomers such as dicyclopentadiene that are provided to obtain high strength polymers [8, 17, 23, 24].

The last two of the above-mentioned approaches are mainly based on the control of the chemistry over choice of monomer and cross-linker, while they are usually implemented using another type of synthetic monomer rather than styrene or DVB. The main drawback in here is being highly dependent on fossil resources. On the other hand, using bio-derived monomers could be a solution both to overcome the disadvantages arises from low mechanical strength and to become undependent on fossil resources. In this respect, there are several sustainable monomers such as norbornene and lactide that can polymerize through ring opening mechanisms. However, terpenes can undergo free radical polymerization and give polymers with isoprene-like building blocks [25].

Terpenes are bio-derived monomer species having one, two, three, or more isoprene units. Myrcene on the other hand is a hydrophobic acyclic monoterpene having three double bonds. As a naturally occurring feedstock, the biocompatibility of this monomer was also approved [26]. Polymerization of myrcene has known to have various benefits such as improving biological and mechanical properties, providing sites for post-functionalization and post-polymerization reactions, as well as producing cross-linked matrices [25]. In this respect, considerable attention has been paid on polymerization and copolymerization reactions of myrcene. Anionic, cationic, coordination, and even controlled and free radical polymerization reactions in different polymerization mediums of this monoterpene were investigated by many scientists [25, 27–32]. However, it was revealed out that free radical polymerization was not as successful as the others due to the hindrance of formation of branching and cross-linking by chain transfer reactions [33–36].

In this study, we aimed to prepare polyHIPE monoliths by free radical copolymerization of β-myrcene. In this respect, we investigated the influence of β-myrcene and selected comonomers on the stability of HIPEs, and as well as on the preparation of cross-linked monoliths. To our knowledge, for the first time in the literature, we have succeeded cross-linking of β-myrcene in the continuous phase of w/o HIPE templates through free radical copolymerization by using a dimethacrylate comonomer.

## Materials and methods

### Materials

β-Myrcene (technical grade, MG International Fragrance Company: Gülçiçek Kimya), 2-ethyl hexyl acrylate (2-EHA; 98%, Sigma-Aldrich), glycidyl methacrylate (GMA; 97%, Sigma-Aldrich), methyl methacrylate (MMA; 99%, Sigma-Aldrich), ethylene glycol dimethacrylate (EGDMA; 98%, Sigma-Aldrich), Pluronic® L121 (poly(ethyleneglycol)-*block*-poly(propyleneglycol)-*block*-poly(ethyleneglycol), Mn ~ 4400, non-ionic surfactant, Aldrich), potassium persulfate (KPS; ≥ 99%, ACS reagent), and calcium chloride hexahydrate ($CaCl_2.6H_2O$; 98%, Sigma-Aldrich) were used as received. In all experiments, ultrapure double distilled deionized water was used.

### HIPE preparation and stability tests

HIPEs were prepared by dispersing 40 mL of internal phase in 10 mL of continuous phase. Continuous phase was prepared by mixing specified amounts of β-myrcene, comonomer (2-EHA, GMA, MMA or EGDMA), and Pluronic® L121 (30 vol% with regard to continuous phase volume) in a round bottom 2-necked reactor equipped with an overhead stirrer. The volume ratio of β-myrcene to comonomer was kept constant at 10/90. Then, the internal phase (deionized water containing 1 wt% of $CaCl_2.6H_2O$) was added by droplets into the continuous phase with the help of a peristaltic pump (pump rate: 50 rpm), under constant stirring (400 rpm). In order to obtain homogeneous distribution of emulsion droplets, stirring was continued for an extra 30 min after the addition of internal phase was completed. Then, the HIPEs were transferred into lidded glass containers. The HIPE consisting of only β-myrcene was also prepared according to the above described method.

Stability tests were performed at two different temperatures. For this purpose, the HIPEs were placed in constant temperature ovens at 25 °C and 60 °C. Then, the stability of the HIPEs was investigated based on the principle of observing phase separation. All tests were continued for 4 weeks.

### PolyHIPE synthesis

In all cases, polyHIPEs were prepared by 80 vol% of nominal porosity. In order to obtain polymerized HIPE monoliths, the same experimental approach described above was used. The only difference from the procedure given above was the preparation of the internal phase by the addition of KPS (1 mol%, with regard to total mole number of the used monomers) in addition to $CaCl_2.6H_2O$. After HIPEs were obtained, they were transferred into glass containers and polymerized at 60 °C by closing the lids. Polymerization was continued

either 24 h or 48 h. After polymerization, resulting monoliths were extracted with ethanol in a Soxhlet apparatus for 24 h and then dried under vacuum at 40 °C until the constant weighing was available.

The influence of the monomer composition was investigated through the formulation resulting in cross-linked polyHIPE monoliths. For this purpose, β-myrcene/comonomer ratio was altered between 10/90 and 90/10 while keeping the other experimental conditions constant. Polymerization at these conditions was continued for 24 h at 60 °C.

## Methods

### Pore morphology

Pore morphology of the polyHIPEs was investigated via scanning electron microscopy (SEM; ZEISS Supra 40 VP, Germany). With this purpose, small pieces taken from the samples were first coated with gold. SEM images were used for the calculation of average cavity sizes (CS) and interconnected pore diameters (IPD). With this respect, at least 100 measurements were taken from the cavities, while more than 180 measurements were taken from the interconnected pores. Then the average diameters were calculated after multiplying each measurement by a correction factor ($2/3^{1/2}$). The statistical error was also determined for each calculation [37].

### Brunauer–Emmet–Teller (BET) surface area

BET surface area ($\delta_{BET}$) of the resulting monoliths was determined by using Micromeritics Gemini VII Surface Area and Porosity Analyzer (Micromeritics Instrument Corporation, USA). Prior to analysis, each sample was prepared for analysis by degassing on Micromeritics FlowPrep 060 Sample Degas Unit (Micromeritics Instrument Corporation, USA). Degassing was continued for 48 h at 25 °C. For each monolith sample, three measurements were taken by using three different specimens. BET surface areas of the monoliths were calculated as the arithmetic average of three measurements.

### Mechanical properties

Since the obtained monoliths were cross-linked polymer foams, mechanical strength was measured against 10 kN compressive force according to the Standard Test Method for Compressive Properties of Rigid Cellular Plastics (ASTM D1621-04a) by using a ZwickRoell Z020 Universal Testing Machine (Zwick GmbH & Co.KG, Germany). Accordingly, stress/strain plots were recorded on a testXpert II Testing Software, and compression modulus was determined from the initial slope of the stress/strain plots. For the mechanical testing of each polyHIPE monolith, five different specimens were synthesized. Testing specimens were used directly after the purification step, without applying any cutting or breaking. Compression modulus was calculated as the arithmetic average of five measurements. Standard error was also calculated for each monolith sample.

## Results and discussion

Preparation of β-myrcene based HIPEs was carried out by using different types of comonomers. For this purpose, comonomers were chosen considering the functional groups, reactivities, and spacer groups. The influence of 2-ethyl hexyl acrylate (2-EHA), glycidyl methacrylate (GMA), methyl methacrylate (MMA), and ethylene glycol dimethacrylate (EGDMA) as comonomer was investigated on the formation of w/o HIPEs. In order to find out the influence of comonomer, internal phase volume and β-myrcene/comonomer ratio, as well as the other emulsification parameters (i.e., addition rate of internal phase, surfactant ratio, mixing rate and time), were kept constant. In each experiment, HIPEs were prepared by using 80 vol% of internal phase, while the ratio of β-myrcene/comonomer was 10/90. In all cases, combining β-myrcene with the selected comonomers resulted in highly stable HIPEs. To investigate the temperature-dependent stabilities of the obtained HIPEs, stability tests were performed at constant temperatures (25 °C and 60 °C) against phase separation. The HIPE, which was prepared by using β-myrcene alone, was also checked. Accordingly, it was determined that the resulting emulsions did not compromise stability at 25 °C during the test. Also, phase separation was not observed for the tested HIPEs for 48 h at 60 °C.

Copolymerization of β-myrcene in w/o type HIPEs with the selected comonomers was also studied. For this purpose, the optimum emulsification and polymerization conditions were kept constant. Copolymerization reactions were carried out using KPS as a radical source. Accordingly, copolymerization reactions were performed at 60 °C for 24 h. Homopolymerization of β-myrcene was also studied at the same experimental conditions. Copolymerization of the HIPE containing β-myrcene and EGDMA in the oil phase was yielded a highly cross-linked polyHIPE monolith. However, copolymerization of β-myrcene with 2-EHA, GMA, and MMA did not yield cross-linked polymers. Homopolymerization of β-myrcene also could not be achieved at the same conditions. For this reason, the influence of increasing the polymerization time was investigated by prolonging the polymerization time of β-myrcene, β-myrcene/2-EHA, β-myrcene/GMA, and β-myrcene/MMA based HIPEs to 48 h. It was observed that the prolonged polymerization time had no significant effect on the cross-linking of emulsion templates. This result might be attributed to the high reactivity of β-myrcene [38] as well as the steric hindrance of consecutive double bonds. Due to its high

reactivity, in most of the cases, growing copolymer chains tend to add β-myrcene, rather than comonomers. On the other hand, high molecular weight homopolymers of poly(β-myrcene)s are also not common due to the increased reversibility of the radical in the propagation step [39]. Despite emulsion templating is a simple approach, the complexity of the medium which is composed of monomers, initiator radicals, emulsifying agent, and high-volume fraction of internal phase has an ultimate effect on the ongoing polymerization reactions. In terms of polymerization kinetics, both the hydrophilicity and the water solubility of the monomers have great importance. Since β-myrcene is quite hydrophobic, it predominantly exists in the continuous phase. Persulfate radicals, on the other hand, are produced in the water phase and diffused to continuous phase through water. Thus, polymerization reaction is expected to proceed at the continuous phase or the interface. In case of homopolymerization of β-myrcene, back reaction for trisubstituted internal double bonds might be predominant. Since poly(β-myrcene)s usually consist four different repeating units (cis- and trans-1,4-; 1,2-; 3,4-units; and stereoisomers), final microstructure of the homopolymer is very complex and determined by the synthetic conditions [39]. On the other hand, addition of monomers to the growing chain radicals depends on the structure of monomers and monomer reactivities, at copolymerization conditions. Considering the phase ratios of HIPEs, monomer polarity and water solubility should also be determinative. We believe that in case of EGDMA, ethylene glycol unit contributes to decreasing the steric hindrance. On the other hand, 2-EHA, GMA, and MMA units might hinder the chains growing or formations of cross-links due to the increased steric hindrance. It is also possible that with the above-mentioned comonomers, β-myrcene tends to add itself as a result of high reactivity, and the predominant back reaction of trisubstituted internal double bonds prevents chain growing. Another probable scenario is that the above-mentioned comonomers act as chain transfer agents in the experimental conditions. This situation might hinder the cross-linking of polymer chains [33–36].

The influence of comonomer composition on the synthesized poly(β-myrcene-*co*-EGDMA) polyHIPEs was investigated in terms of morphological, mechanical, and thermal properties. With this aim, β-myrcene/EGDMA ratio was altered between 10/90 and 90/10. In all cases, stable HIPEs were obtained, and copolymerization of each HIPE template resulted in solid monoliths. Resulting monoliths were termed as PMyE-x, in which x is denoting the order of experiments and β-myrcene ratio.

Morphology of the PMyE-x monoliths was investigated via SEM imaging. To make a meaningful comparison and demonstrate the presence of β-myrcene on the final properties, polyEGDMA (PEGDMA) monolith was also synthesized. The pore morphology of PEGDMA is presented in Fig. 1a, while SEM images of PMyE-x monoliths are presented in Fig. 1b–j. According to the SEM image given in Fig. 1a, PEGDMA monolith exhibits cauliflower morphology. Previous studies in the literature have shown that the same trend was observed also with the polymerization of HIPEs based on polar functional monomers such as EGDMA [14, 40], MMA [14, 15], and GMA [41]. It was suggested that the cauliflower morphology was observed in the case of using a reaction mixture composed of monomer, cross-linker, initiator, and porogen. The basis of this suggestion is relied on the solubility of polymer chains in porogenic solvents. There are also some examples of monoliths with similar morphologies obtained without the use of porogenic solvents [14, 40]. However, the appearance of cauliflower morphology can be explained by the solubility of the growing polymer chains in general. By polymerization, solubility of the growing chains in the reaction mixture decreases with the increase of polymer chain length. Afterwards, polymer chains precipitate and form nuclei. It is known that thermodynamically a monomer is a good solvent for its polymer. In the later stages of polymerization, precipitated polymer nuclei start to be swollen with its own monomer. At this point, the concentration of monomer molecules in the surrounding reaction mixture is lower than the concentration in the nuclei. Consequently, polymerization in the nuclei is kinetically preferred. In the end, first microglobules are formed due to the increment of the size of nuclei, and then these microglobules formed clusters as a result of aggregation. The cauliflower morphology is suggested to be the result of the cross-linking of grown microglobules [42–44].

Comparison of the SEMs given in Fig. 1 reveals that the unique polyHIPE morphology consisting of cavities connected through interconnected pores only occurred for the β-myrcene ratios lower than 70 vol%. For the comonomer ratios changing between 10/90 and 50/50, resulting monoliths were exhibiting a highly open porous morphology. However, the number of the interconnected pores significantly decreased for the monolith sample pMyE-6, while pMyE-7 sample was exhibiting fully closed-cell morphology.

For the monoliths in which β-myrcene was higher than 70 vol% (PMyE-8 and PMyE-9), significant amount of volume contraction was observed after drying of the solvent extracted samples. In addition, it was determined that these monoliths had a distinctive rubbery behavior and exhibited reversible deformation. However, the SEM images given in Fig. 1i and j revealed that the cavities were fully collapsed in these samples. It is known that the voids of a polyHIPE are formed as a result of the continuous polymer film formation around the emulsion droplets during polymerization, and the interconnected pores are formed as a result of volume contraction accompanying the conversion of monomer units into polymer chains [10]. Consequently, the collapse of the pore topology can be thought to be the result of β-myrcene's free radical polymerization kinetics. At higher β-myrcene ratios,

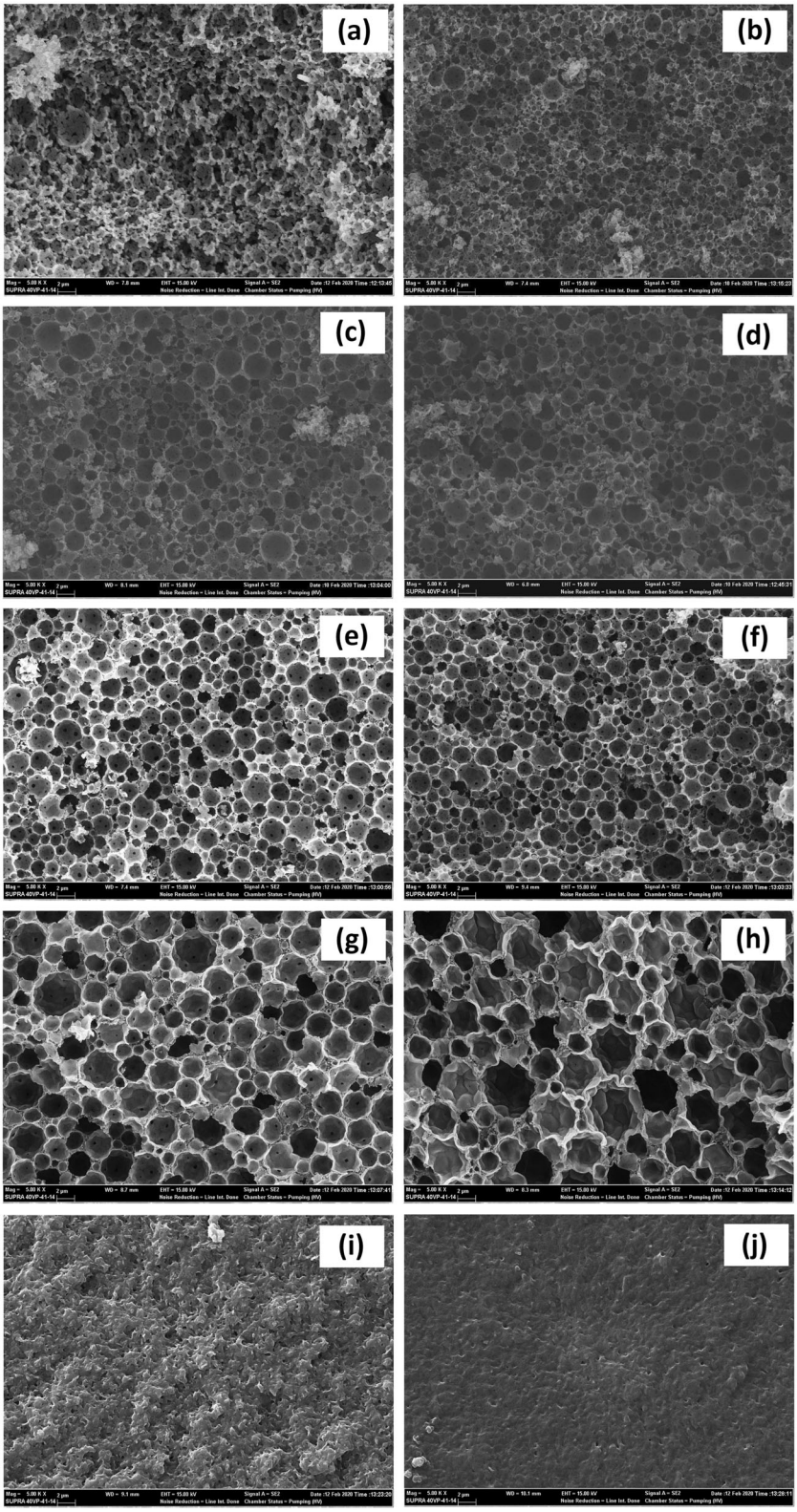


**Fig. 1** SEM images of the polyHIPE monoliths: (**a**) PEGDMA, (**b**) PMyE-1, (**c**) PMyE-2, (**d**) PMyE-3, (**e**) PMyE-4, (**f**) PMyE-5, (**g**) PMyE-6, (**h**) PMyE-7, (**i**) PMyE-8, and (**j**) PMyE-9

addition of EGDMA monomer to growing chains or the cross-linking of chains may have prevented. Another probability might be the change of interfacial tension due to the increase of $\beta$-myrcene amount. Within the frame of this probability, one can also say that the surfactant used does not function enough, at these conditions.

On the other hand, it was observed that the cavity structures were also highly related to the monomer ratios. While the

**Table 1** Morphological properties and compression moduli of the polyHIPE monoliths

| Sample | β-Myrcene/ EGDMA | CS (μm) | IPD (μm) | $\delta_{BET}$ ($m^2g^{-1}$) | CM (MPa) |
|---|---|---|---|---|---|
| PMyE-1 | 10:90 | 1.12 ± 0.04 | 0.19 ± 0.01 | 36.04 | 34.20 ± 0.42 |
| PMyE-2 | 20:80 | 1.09 ± 0.03 | 0.15 ± 0.00 | 34.45 | 34.80 ± 0.97 |
| PMyE-3 | 30:70 | 2.41 ± 0.06 | 0.24 ± 0.01 | 32.41 | 37.10 ± 1.66 |
| PMyE-4 | 40:60 | 2.08 ± 0.05 | 0.31 ± 0.01 | 24.70 | 38.80 ± 0.57 |
| PMyE-5 | 50:50 | 2.30 ± 0.09 | 0.31 ± 0.01 | 21.81 | 34.80 ± 0.38 |
| PMyE-6 | 60:40 | 3.19 ± 0.15 | 0.30 ± 0.01 | 16.51 | 18.70 ± 0.61 |
| PMyE-7 | 70:30 | 3.55 ± 0.19 | – | 8.56 | 11.20 ± 0.15 |
| PMyE-8 | 80:20 | – | – | 4.27 | 5.57 ± 0.03 |
| PMyE-9 | 90:10 | – | – | 0.07 | 0.15 ± 0.00 |
| PEGDMA | – | 1.91 ± 0.09 | 0.39 ± 0.01 | 18.08 | 9.65 ± 0.09 |

shape of cavities was spherical for the monoliths having β-myrcene ratios lower than 60 vol%, polyHIPEs prepared with β-myrcene ratios of 60 and 70 vol% were found to have cavities more like polyhedral than spherical. In addition, for the open porous monoliths, interconnected pores were almost perfectly spherical. As reported in the literature, this pore morphology can be attributed to the locus of initiation. In the presence of a water-soluble initiator, HIPE polymerization is mostly expected to be initiated at the interface. In the interfacial initiation, the thin film between two adjacent water droplets stabilized at the interface and the water-soluble initiator ensure polymerization on droplets and lead to the formation of flat films which resulted in closed-cell polyhedral structure. However, polymerization is initiated in the bulk phase in the presence of an oil-soluble initiator, and the thin film formed between the adjacent water droplets is teared to give an open-cell spherical morphology. [2, 45–49]. In this study, as well as a water-soluble soluble initiator was used in all cases, formation of closed-cell polyhedral pores was observed only after a critical monomer ratio was exceeded. This result implies that HIPEs are stable when the β-myrcene ratio was less than 60 vol%. This situation might be explained by the hydrohilic/lyphophilic balance of the continuous phase and the function of the used surfactant (Pluronic® L121). Since β-myrcene has a highly hydrophobic structure on the contrary to EGDMA, it can be thought that stabilizing ability of the surfactant was reduced at higher β-myrcene ratios. At low β-myrcene ratios, as a result of the higher stabilizing function of the surfactant, it can be thought that the polymerization mainly continued in the continuous phase. Thereby, open-cell monoliths with spherical cavities are formed. Once the ratio of β-myrcene exceeded a critical limit, the soluble radicals in the aqueous phase are located at the interface, and the locus of initiation shifts to the interface. As a result, at these conditions, obtained polyHIPEs have higher average cavity sizes. In addition, pore morphology has turned into polyhedral

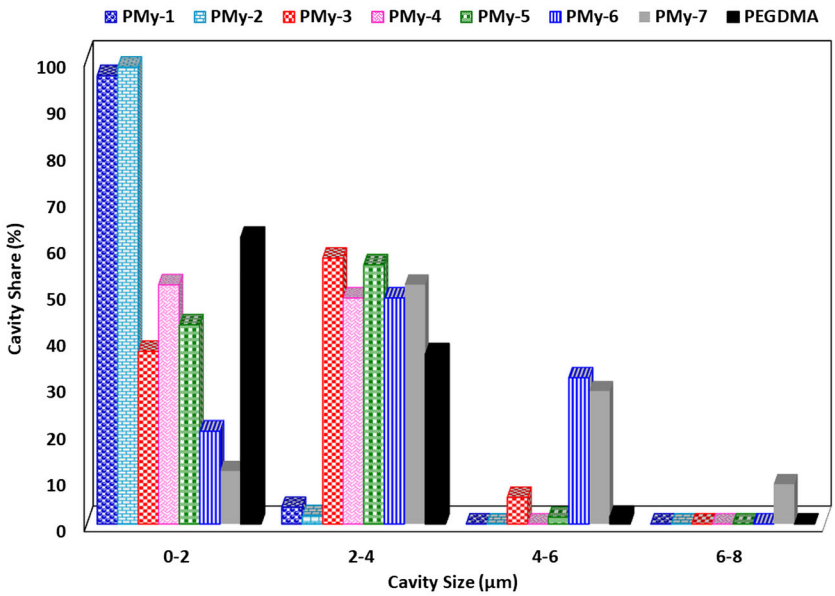


**Fig. 2** Share of cavities for the polyHIPE monoliths

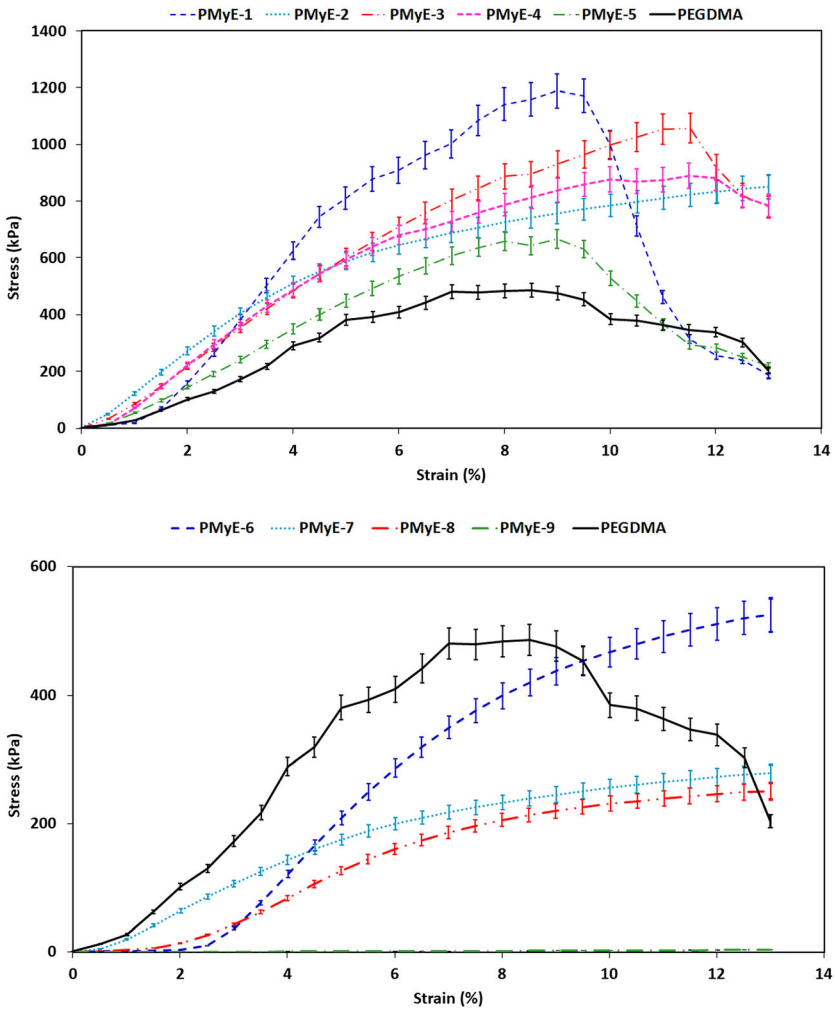


**Fig. 3** Stress/strain plots of the polyHIPE monoliths

closed-cell morphology from spherical open-cell. The reader should be reminded that we prepared all HPEs in this by using 30 vol% Pluronic® L121 and 1 mol% of KPS. We believe that the pore morphology and openness can be altered by using surfactant mixtures. It is also possible to control the polymer film rupture by preventing the rapid polymerization [47, 50]. We will discuss this in a follow-up paper.

SEM images were also used for the calculation of average cavity size (CS) and interconnected pore diameter (IPD). Calculated data were presented in Table 1. According to Table 1, average cavity size of PMyE-x monoliths was altering between 1.09 and 3.55 μm, while interconnected pore diameter was ranging between 0.15 and 0.31 μm. As compared with PEGDMA monolith, addition of *β*-myrcene first decreases the average cavity size. With the increasing *β*-myrcene ratio in the continuous phase, average cavity size of the resulting monoliths was also increased. It was observed that for the samples having 10 and 20 vol% of *β*-myrcene, variation of cavity size was negligible. As mentioned above, the variation of cavity size becomes distinctive by exceeding the critical *β*-myrcene ratio. It can be concluded by considering the SEM images given in Fig. 1 that the change of the cavity size should be evaluated together with the geometry of the cavities.

Cavity share graph presented in Fig. 2 reveals the narrow cavity size distribution especially for PMyE-1 and PMyE-2 monoliths. According to cavity size distribution calculations, respectively, 96% and 98% of the cavities of these monolith samples are changing between 0 and 2 μm. It is observed that the monomer ratio has an important effect, also on the cavity size distribution. It can be seen from Fig. 2 that cavity size distribution was altered with the increasing ratio of *β*-myrcene. In monoliths where the ratio of *β*-myrcene varies between 30 and 50 vol%, it is seen that the cavities were distributed between 0–2 and 2–4 μm. However, monoliths prepared by using 60 vol% and 70 vol% of β-myrcene were found to have wider cavity size distribution. In addition, interconnected pore sizes increased with increasing amount of *β*-myrcene as compared with the neat PEGDMA monolith. However, when the ratio of comonomers reached to 50/50, the increment of the interconnected pore sizes has also stopped.

BET specific surface area ($\delta_{BET}$) of the obtained monoliths was measured through $N_2$ adsorption/desorption analysis. For this purpose, BET equation was applied to the $N_2$ isotherms of the monolith samples. It was found that the specific surface area of the PMyE-x monoliths rapidly decreased with the increasing ratio of β-myrcene. In addition, variation of the specific surface area was found to be coherent with the variation of average cavity sizes.

Mechanical strength of the resulting monoliths was investigated against 10 kN compression load. The compression modulus (CM) of each monolith was determined from the initial slope of the stress/strain plots that were presented in Fig. 3. In order to demonstrate the influence of β-myrcene on the compressive strength, the neat PEGDMA monolith was also tested for comparison. It can be seen from the compression modulus data presented in Table 1 that β-myrcene significantly improved the compressive strength of the polyHIPE monoliths. Replacing even 10 vol% of EGDMA monomer by myrcene in the formulation leads compression modulus to increase at a ratio as high as 254.4%. Moreover, it has been observed that the increase in the compression modulus continues to increase until the β-myrcene/EGDMA ratio is 50/50. With the increase of myrcene ratio up to 60 vol%, a significant decrement was observed in compression modulus. Accordingly, decrement of compression modulus continued with the increasing ratio of β-myrcene for the monolith samples PMyE-7, PMyE-8, and PMyE-9. Even though the PMyE-8 and PMyE-9 exhibit reversible deformation, these monoliths have shown the lowest compressive strength.

## Conclusion

In summary, it was demonstrated that β-myrcene can be used as a renewable monomer for the preparation of polyHIPE monoliths having relatively improved mechanical strength accompanied with narrow cavity size distribution. In addition, the importance of reaction kinetics at the copolymerization of β-myrcene with conventional monomers was emphasized. It was shown that myrcene was only copolymerized with EGDMA, which has an ethylene glycol spacer group.

Morphological and mechanical investigations showed that final properties of the polyHIPE monoliths can be tailored by changing the monomer composition. It was found that β-myrcene has a positive contribution on the mechanical properties due to its isoprene units. Brittleness of the obtained polyHIPE monoliths had reduced thanks to the rubbery-like behavior of polymerized β-myrcene and of course the contribution of flexible EGDMA units. 50/50 monomer ratio has also been found to be the critical monomer composition for the determination of optimum morphological and mechanical properties. In addition, it was also concluded that for the preparation of β-myrcene polyHIPEs to be used in various applications, experimental parameters, such as internal phase ratio, surfactant type and amount, and polymerization rate, should also be investigated comprehensively. In a follow-up work, we will elaborate on the relation between these experimental parameters and pore morphology.

**Acknowledgments** Authors thank the MG International Fragrance Company, Gülçiçek Kimya (Gebze, Kocaeli, Turkey), for their kind donation of β-myrcene.

## Compliance with ethical standards

**Conflict of interest** The authors declare that they have no conflict of interest.

## References

1. Silverstein MS (2020) The chemistry of porous polymers: the holey grail. Isr J Chem 60:1–12. https://doi.org/10.1002/ijch.202000003
2. Zhang T, Sanguramath RA, Israel S, Silverstein MS (2019) Emulsion templating: porous polymers and beyond. Macromolecules 52:5445–5479. https://doi.org/10.1021/acs.macromol.8b02576
3. Zhang T, Zhao Y, Silverstein MS (2020) Cellulose-based, highly porous polyurethanes templated within non-aqueous high internal phase emulsions. Cellulose 27:4007–4018. https://doi.org/10.1007/s10570-020-03059-z
4. David D, Silverstein MS (2009) Porous polyurethanes synthesized within high internal phase emulsions. J Polym Sci A Polym Chem 47:5806–5814. https://doi.org/10.1002/pola.23624
5. Naranda J, Sušec M, Maver U, Gradišnik L, Gorenjak M, Vukasović A, Ivković A, Rupnik MS, Vogrin M, Krajnc P (2016) Polyester type polyHIPE scaffolds with an interconnected porous structure for cartilage regeneration. Sci Rep 6:28695. https://doi.org/10.1038/srep28695
6. Gurevitch I, Silverstein MS (2011) Nanoparticle-based and organic-phase-based AGET ATRP polyHIPE synthesis within Pickering HIPEs and surfactant-stabilized HIPEs. Macromolecules 44:3398–3409. https://doi.org/10.1021/ma200362u
7. Khodabandeh A, Dario Arrua R, Desire CT, Rodemann T, Bon SAF, Thickett SC, Hilder EF (2016) Preparation of inverse polymerized high internal phase emulsions using an amphiphilic macro-RAFT agent as sole stabilizer. Polym Chem 7:1803–1812. https://doi.org/10.1039/C5PY02012C
8. Mert EH, Slugovc C, Krajnc P (2015) Tailoring the mechanical and thermal properties of dicyclopentadiene polyHIPEs with the use of a comonomer. eXPRESS Polym Lett 9:344–353. https://doi.org/10.3144/expresspolymlett.2015.32
9. Yüce E, Mert EH, Krajnc P, Parın FN, San N, Kaya D, Yıldırım H (2017) Photocatalytic activity of titania/polydicyclopentadiene polyHIPE composites. Macromol Mater Eng 302:1700091. https://doi.org/10.1002/mame.201700091
10. Pulko I, Krajnc P (2017) Porous polymer monoliths by emulsion templating. Encyclopedia of Polymer Science and Technology, Wiley. https://doi.org/10.1002/0471440264.pst653
11. Barby D, Haq Z (1982) Low density porous cross-linked polymeric materials and their preparation. Eur Patent 0060138
12. Cameron NR (2005) High internal phase emulsion templating as a route to well-defined porous polymers. Polymer 46:1439–1449. https://doi.org/10.1016/j.polymer.2004.11.097

13. Mert HH, Mert MS, Mert EH (2019) A statistical approach for tailoring the morphological and mechanical properties of polystyrene polyHIPEs: looking through experimental design. Mater Res Express 6:1153006. https://doi.org/10.1088/2053-1591/ab437f
14. Yüce E, Parın FN, Krajnc P, Mert HH, Mert EH (2018) Influence of titania on the morphological and mechanical properties of 1,3-butanediol dimethacrylate based polyHIPE composites. React Func Polym 130:8–15. https://doi.org/10.1016/j.reactfunctpolym.2018.05.009
15. Paljevac M, Kotek J, Jeřabek K, Krajnc P (2018) Influence of topology of highly porous methacrylate polymers on their mechanical properties. Macromol Mater Eng 303:1700337. https://doi.org/10.1002/mame.201700337
16. Menner A, Salgueiro M, Shaffer MSP, Bismarck A (2008) Nanocomposite foams obtained by polymerization of high internal phase emulsions. J Polym Sci Part A Polym Chem 46:5708–5714. https://doi.org/10.1002/pola.22878
17. Yüce E, Krajnc P, Mert HH, Mert EH (2019) Influence of nanoparticles and antioxidants on mechanical properties of titania/polydicyclopentadiene polyHIPEs: a statistical approach. J Appl Polym Sci 136:46913. https://doi.org/10.1002/app.46913
18. Berber E, Çira F, Mert EH (2016) Preparation of porous polyester composites via emulsion templating: investigation of the morphological, mechanical, and thermal properties. Polym Compos 37:1531–1538. https://doi.org/10.1002/pc.23323
19. Wu R, Menner A, Bismarck A (2010) Tough interconnected polymerized medium and high internal phase emulsions reinforced by silica particles. J Polym Sci Part A Polym Chem 48:1979–1989. https://doi.org/10.1002/pola.23965
20. Çira F, Mert EH (2015) PolyHIPE/Pullulan composites derived from glycidyl methacrylate and 1,3-butanediol dimethacrylate-based high internal phase emulsions. Polym Eng Sci 55:2636–2642. https://doi.org/10.1002/pen.24156
21. Huš S, Kolar M, Krajnc P (2015) Tailoring morphological features of cross-linked emulsion-templated poly(glycidyl methacrylate). Des Monomers Polym 18:698–703. https://doi.org/10.1080/15685551.2015.1070503
22. Huš S, Krajnc P (2015) PolyHIPEs from methyl methacrylate: hierarchically structured microcellular polymers with exceptional mechanical properties. Polymer 55:4420–4424. https://doi.org/10.1016/j.polymer.2014.07.007
23. Kovačič S, Matsko NB, Ferk G, Slugovc C (2013) Macroporous poly(dicyclopentadiene) $\gamma Fe_2O_3/Fe_3O_4$ nanocomposite foams by high internal phase emulsion templating. J Mater Chem A 1:7971–7978. https://doi.org/10.1039/C3TA11402C
24. Vakalopoulou E, Slugovc C (2019) The effects of enhancing the crosslinking degree in high internal phase emulsion templated poly(dicyclopentadiene) cured by ring-opening metathesis polymerization by a crosslinking comonomer. Macromol Chem Phys 220:1900423. https://doi.org/10.1002/macp.201900423
25. Bauer N, Brunke J, Kali G (2017) Controlled radical polymerization of myrcene in bulk: mapping the effect of conditions on the system. ACS Sustain Chem Eng 5:10084–10092. https://doi.org/10.1021/acssuschemeng.7b02091
26. Behr A, Johnen L (2009) Myrcene as a natural base chemical in sustainable chemistry: a critical review. Chem Sus Chem 2:1072–1095. https://doi.org/10.1002/cssc.200900186
27. Métafiot A, Kanawati Y, Gérard JF, Defoort B, Marić M (2017) Synthesis of β-myrcene-based polymers and styrene block and statistical copolymers by SG1 nitroxide-mediated controlled radical polymerization. Macromolecules 50:3101–3120. https://doi.org/10.1021/acs.macromol.6b02675
28. Yang X, Li S, Xia J, Song J, Huang K, Li M (2015) Renewable myrcene-based-UV-curable monomer and its copolymers with acrylated epoxidized soybean oil: design, preparation, and characterization. Bioresources 10:2130–2142. https://doi.org/10.15376/biores.10.2.2130-2142
29. Johanson AJ, Mckennon FL, Goldblatt LA (1948) Emulsion polymerization of myrcene. Ind Eng Chem 40:500–502. https://doi.org/10.1021/ie50459a033
30. Loughmari S, Hafid A, Bouazza A, El Bouadili A, Zinck P, Visseaux M (2012) Highly stereoselective coordination polymerization of β-myrcene from a lanthanide-based catalyst: access to bio-sourced elastomers. J Polym Sci Part A Polym Chem 50:2898–2905. https://doi.org/10.1002/pola.26069
31. Metafiot A, Gérard JF, Defoort B, Marić M (2018) Synthesis of β-myrcene/glycidyl methacrylate statistical and amphiphilic diblock copolymers by SG1 nitroxide-mediated controlled radical polymerization. J Polym Sci Part A Polym Chem 56:860–878. https://doi.org/10.1002/pola.28963
32. Hilschmann J, Kali G (2015) Bio-based polymyrcene with highly ordered structure via solvent free controlled radical polymerization. Eur Polym J 73:363–373. https://doi.org/10.1016/j.eurpolymj.2015.10.021
33. Cawse JL, Stanford JL, Still RH (1986) Polymers from renewable sources. III. Hydroxy-terminated myrcene polymers. J Appl Polym Sci 31:1963–1975. https://doi.org/10.1002/app.1986.070310702
34. Cawse JL, Stanford JL, Still RH (1986) Polymers from renewable sources. IV. Polyurethane elastomers based on myrcene polyols. J Appl Polym Sci 31:1549–1565. https://doi.org/10.1002/app.1986.070310602
35. Cawse JL, Stanford JL, Still RH (1987) Polymers from renewable sources: 5. Myrcene-based polyols as rubber-toughening agents in glassy polyurethanes. Polymer 28:368–374. https://doi.org/10.1016/0032-3861(87)90187-X
36. Still RH, Cawse JL, Stanford J (1984) Functionally Terminated Polymers from Terpene Monomers and Their Applications. US Patent 4564718
37. Barbetta A, Cameron NR (2004) Morphology and surface area of emulsion-derived (polyHIPE) solid foams prepared with oil-phase soluble porogenic solvents: span 80 as surfactant. Macromolecules 37:3188–3201. https://doi.org/10.1021/ma0359436
38. Trumbo DL (1993) Free radical copolymerization behavior of myrcene I. copolymers with styrene, methyl methecrylate or p-fluorostyrene. Polym Bull 31:629–636. https://doi.org/10.1007/BF00300120
39. Matic A, Schlaad H (2018) Thiol-ene photofunctionalization of 1,4-polymyrcene. Polym Int 67:500–505. https://doi.org/10.1002/pi.5534
40. Krajnc P, Lebera N, Štefanec D, Kontrec S, Podgornik A (2005) Preparation and characterisation of poly(high internal phase emulsion) methacrylate monoliths and their application as separation media. J Chrom A 1065:69–73. https://doi.org/10.1016/j.chroma.2004.10.051
41. Barbetta A, Dentini M, Leandri L, Ferraris G, Coletta A, Bernabei M (2009) Synthesis and characterization of porous glycidyl methacrylate–divinylbenzene monoliths using the high internal phase emulsion approach. React Funct Polym 69:724–736. https://doi.org/10.1016/j.reactfunctpolym.2009.05.007
42. Vlakh EG, Tennikova TB (2007) Preparation of methacrylate monoliths. J Sep Sci 30:2801–2813. https://doi.org/10.1002/jssc.200700284
43. Peters EC, Svec F, Fréchet JMJ (1997) Preparation of large-diameter "molded" porous polymer monoliths and the control of pore structure homogeneity. Chem Mater 9:1898–1902. https://doi.org/10.1021/cm970204n
44. Strancar A, Podgornik A, Barut M, Necina R (2002) Short monolithic columns as stationary phases for chromatography. In: Scheper T (ed) Advances in Biochemical Engineering & Biotechnology 76. Springer-Verlag, Berlin-Heidelberg, pp 49–85

45. Luo Y, Wang AN, Gao X (2015) One-pot interfacial polymerization to prepare polyHIPEs with functional surface. Colloid Polym Sci 293:1767–1779. https://doi.org/10.1007/s00396-015-3567-y
46. Robinson JL, Moglia RS, Stuebben MC, McEnery MAP, Cosgriff-Hernandez E (2014) Achieving interconnected pore architecture in injectable polyHIPEs for bone tissue engineering. Tissue Eng Part A 20:1103–11012. https://doi.org/10.1089/ten.tea.2013.0319
47. Quell A, Bergolis B, Drenckhan W, Stubenrauch C (2016) How the locus of initiation influences the morphology and the pore connectivity of a monodisperse polymer foam. Macromolecules 49:5059–5067. https://doi.org/10.1021/acs.macromol.6b00494
48. Stubenrauch C, Menner A, Bismarck A, Drenckhan W (2018) Emulsion and foam templating—promising routes to tailor-made porous polymers. Angew Chem Int Ed 57:10024–10032. https://doi.org/10.1002/anie.201801466
49. Rezanavaz R, Fee CJ, Dimartino S (2018) GMA-based emulsion-templated solid foams: influence of co-crosslinker on morphology and mechanical properties. J Appl Polym Sci 135:46295. https://doi.org/10.1002/APP.46295
50. Wu R, Menner A, Bismarck A (2013) Macroporous polymers made from medium internal phase emulsion templates: effect of emulsion formulation on the pore structure of polyMIPEs. Polymer 54:5511–5517. https://doi.org/10.1016/j.polymer.2013.08.029